

1 **Reuse of Abandoned Oil and Gas Wells for Geothermal Energy Production**

2

3

Robert Caulk¹, M.Sc. and Ingrid Tomac², Ph.D.

4

¹Graduate Research Assistant, Department of Structural Engineering, University of California,
6San Diego, La Jolla, CA 92093-0085; email: rcaulk@eng.ucsd.edu

²Research Scientist, Department of Structural Engineering, University of California, San Diego,
8La Jolla, CA 92093-0085; email: itomac@eng.ucsd.edu

9

10**ABSTRACT**

11

12This paper presents an investigation on the suitability of abandoned wells in California for
13Enhanced Geothermal Systems (EGS) and low temperature deep Borehole Heat Exchanger
14(BHE) applications. The study identifies three counties characterized by high numbers of
15abandoned wells, medium to high crustal heat flows (75-100 mW/m²), and suitable sedimentary
16geology: Santa Clara, Monterey, and Santa Barbara. Thermal gradients range between 4 and 7.3
17°C /100 m and enable access to the bottom hole temperatures between 40-73 °C for an average
181,000 m deep well. These rock temperatures are sufficient for low-temperature direct use EGS
19such as district heating, greenhouse heating, and aquaculture. Abandoned wells reuse mitigation
20of drilling costs and the documented lithology both reduce the risk associated with EGS.
21However, hydraulic fracturing of loosely to moderately consolidated sedimentary rock in
22transitional stress regimes remains one limitation to the EGS conversion of these abandoned
23wells. The feasibility of deep BHE applications within abandoned oil and gas wells is
24demonstrated here by a mathematical model. Predictions show that outlet fluid temperatures >40
25°C can be achieved for 1,000 m deep wells in regions with temperature gradients >7 °C /100 m.

26

27Keywords: Geothermal, abandoned well, hydraulic fracturing, BHE, heat flow, California

28

29Preprint submitted to *Renewable Energy*

March 27, 2017

30

31

321. INTRODUCTION

33The objective of this paper is to investigate the prospect of using abandoned oil and gas wells in
34the state of California for harvesting geothermal energy. According to well data documented and
35maintained by the California Department of Conservation, Division of Oil and Gas and
36Geothermal Resources (DOGGR) there are approximately 147,127 wells currently indicated as
37abandoned, plugged, buried, and/or inactive. Santa Barbara County alone hosts 5,184 of these
38unused wells (DOGGR 2016). Most of the wells were plugged due to a decline of oil and gas
39productivity, while other wells were exploratory. In both cases, the existing wells provide
40valuable subsurface information such as lithology, temperature, and formation porosity.
41Augustine et al. (2006) showed that wells drilled to 5 km in 2003 cost ca. 5 million dollars each.
42Considering that drilling costs account for 42%-95% of total Enhanced Geothermal System
43(EGS) power plant costs (Tester et al. 1994), the pre-drilled and extendable abandoned wells may
44prove extremely valuable.

45 Geothermal heat has been traditionally extracted at locations characterized by
46hydrogeological anomalies, but recent advances in engineering have enabled development of
47alternative approaches such as are EGS and borehole heat exchangers (BHE). Both EGS and
48BHE technologies harvest Earth's heat without the location constraints of hydrothermal systems.
49Enhanced Geothermal Systems (EGS) produce electrical energy by enhancing in-situ
50permeability and harvesting heat from hot rock geo-reservoirs. Crustal heat is mined by the
51injection and permeation of cold fluid through hot rock. Heat is transferred from rock to fluid
52and ultimately recovered through a production well. The connection between injection and
53production wells is engineered either by hydraulic fracturing of continuous rock mass or by
54hydro-shearing of existing fractures in the rock (Tester et al. 2006; Economides 2000). The most
55important factors which influence the viability of an EGS are fluid flow rate and temperature.
56Flow rates and temperatures of existing EGS range from 15 to 430 l/s and 40 to 250 °C, where
57higher flow rates and temperatures support power generation and lower values support direct hot
58water use (Li and Lior 2014). EGS flow rates can be increased via georeservoir permeability
59stimulation, but temperatures can only be increased by drilling deeper in to the Earth's crust.
60Crustal temperature depends on crustal heat flow, where temperatures increase with the presence
61of insulating rock layers and magma chambers. Different from EGS, BHEs harvest geothermal
62energy without allowing working fluid to contact soil or rock. Instead, BHEs use various closed

63loop configurations for circulating working fluid through pipes buried in the subsurface, while
64exchanging thermal energy with the soil. Shallow BHEs extend 50-200 m into the earth and are
65usually coupled with Ground Source Heat Pumps (GSHP) to exploit the subsurface as a thermal
66source/sink during winter/summer for residential and commercial heating and cooling (Lund and
67Boyd 2016). Deep BHEs invoke the same principles as shallow BHEs but they reach depths of
681000 to 3000 m where rock temperatures can exceed 85 °C and raw produced fluid temperatures
69range from 20-55 °C (Spinska-Silwa et al. 2015). Like EGS, the production fluid temperature of a
70deep BHE strongly depends on crustal heat flow. Different from EGS, the efficiency of deep
71BHEs depend on heat exchanger configuration and the host rock thermal properties (Dijkshoorn
72et al. 2013) instead of hydraulic properties such as porosity and permeability. In fact, heat
73exchanger insulation design/cost may determine deep BHE project feasibility (Śliwa and Kotyza,
742000; Dijkshoorn et al. 2013). Table 1 lists some existing deep BHEs in Germany and
75Switzerland. These examples make use of a coaxial tube configuration consisting of two
76concentric tubes: one carrying fluid down and the other carrying fluid backup through the center.
77This deep BHE configuration has been investigated and proven viable in various locations
78around Europe (Śliwa, Rosen and Jezuit 2014).

79

80**Table 1.** Existing Deep BHE sites

Site, Country	Peaking method	EWT ¹ °C	Depth (m)	Flow rate (l/s)
Aachen, Germany (<i>Dijkshoorn et al 2013</i>)	Heat pump	25-55	2,500	2.77
Prenzlau, Germany (<i>Schnieder et al. 1996</i>)	Heat pump and Gas/oil boiler	-	2,786	6
Weissbad, Switzer. (<i>Kohl et al 2000</i>)	Heat pump	15	1,200	2.9
Weggis, Switzer. (<i>Kohl et al 2002</i>)	Heat pump	40	2,300	0.8-1.75

81¹Entering Water Temperature (outlet temp from abandoned well heat exchanger)

82

83 EGS and deep BHE geothermal energy extraction technologies couple well with specific
84recreational and industrial applications. In many countries 40 °C geothermal water sources are
85used to heat recreational pools and residential houses, while industrial uses for 40 to 70 °C water
86include aquaculture, greenhouse heating, water desalination and district heating (Bai et al. 2010).
87Although an effective district heating system requires fluid temperature of 40 °C (Lund and

88Lineau 1997), lower water temperatures (ca. 23 °C) combined with locally installed heat pumps
89is a viable alternative (Kulcar et al. 2008; Østergaard and Lund 2011). Several examples of
90geothermal based district heating can be found in Iceland, France, Poland, Hungary, Turkey, and
91the USA. To illustrate the range of BHE capacity, a district heating system in Idaho, USA heats
924000 homes while another system in Reykjavik, Iceland provides heat to 35000 homes using an
9385 °C source and 1850 l/s (Lund and Lienau 1997).

94 The economic viability of EGS and deep BHEs depends on a variety of factors including
95prospecting technologies, drilling technologies, reservoir technologies, energy costs in the
96region, resource longevity, etc. (Tester et al. 2000). The reuse of abandoned wells removes
97prospecting and drilling risks, but the remaining factors still require focused research. For
98example, fracture network stimulation in a sedimentary reservoir requires different procedures
99compared to a similar network design in an igneous reservoir due to differences in fluid
100migration, pore pressures, and cementation/crystallization (Economides, 2000). While the
101economic viability of EGS remains a research topic, deep BHEs stem from well-established
102shallow BHE technologies (Lund and Boyd, 2015). Without a dependence on uncertain fracture
103networks, the economic viability of deep BHEs depends almost entirely on comparable regional
104energy prices (Śliwa and Kotyza, 2003). The same study concluded that plugging an abandoned
105well may, in some cases, be more expensive than refurbishing it for thermal extraction. Further, a
106deep coaxial BHE configuration doubles as a “maintained” plug for abandoned wells, since the
107efficiency of the deep coaxial BHE depends on the continuity of the cement in the casing-rock
108annulus. This requirement reduces the chance for oil/gas migration to the surface or into aquifers.
109Another study performed on the reuse of abandoned oil wells in Carpathians, Poland concluded
110that the benefits were ubiquitous with the only downside being the challenging optimization of
111design parameters (Śliwa, Rosen and Jezuit 2014). Another economic benefit of retrofitting
112abandoned oil and gas wells is the large number of identified drilled wells. While one single deep
113BHE well may not be sufficient to harvest energy equivalent of the relatively larger scale EGS
114reservoirs, thousands of BHE wells may have comparable scale.

115 This paper focuses on the reuse of abandoned oil and gas wells situated in predominantly
116sandstone and shale rock formations at depths of 900 to 2000 m. Based on the available data for
117crustal heat flow with depth, many of the existing wells may be deepened to produce electricity
118by exploiting >100 °C rock. Alternatively, it is possible to directly use lower temperature fluids

119(20-40 °C) for recreational, industrial, agricultural and residential applications. The aim of this
120study is to investigate the feasibility of EGS and deep BHE installations in abandoned wells
121throughout California. Since deep BHE installations are well studied in other countries, a physics
122based model was constructed for the range of well depths and crustal thermal gradients that were
123encountered in Santa Barbara, Santa Clara, and Monterey. The goal of the deep BHE model is to
124estimate the necessary abandoned well depths and thermal gradients associated with 40 °C
125production fluid temperatures.

1262. CALIFORNIA ABANDONED WELLS CHARACTERISTICS

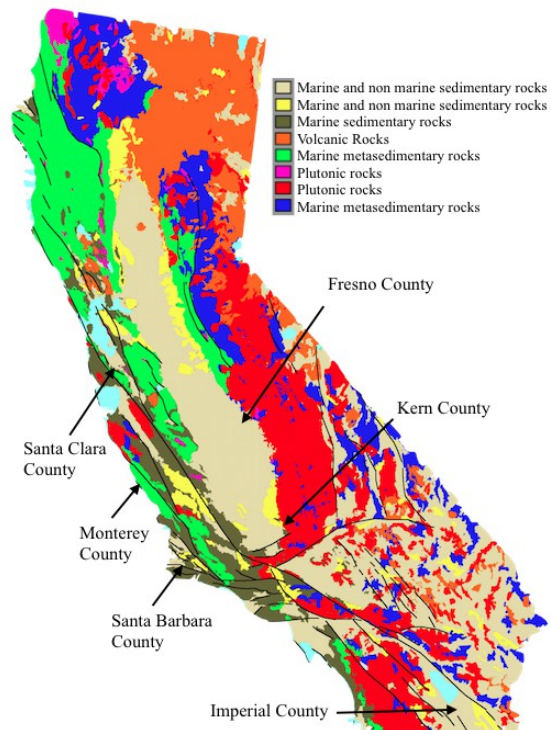
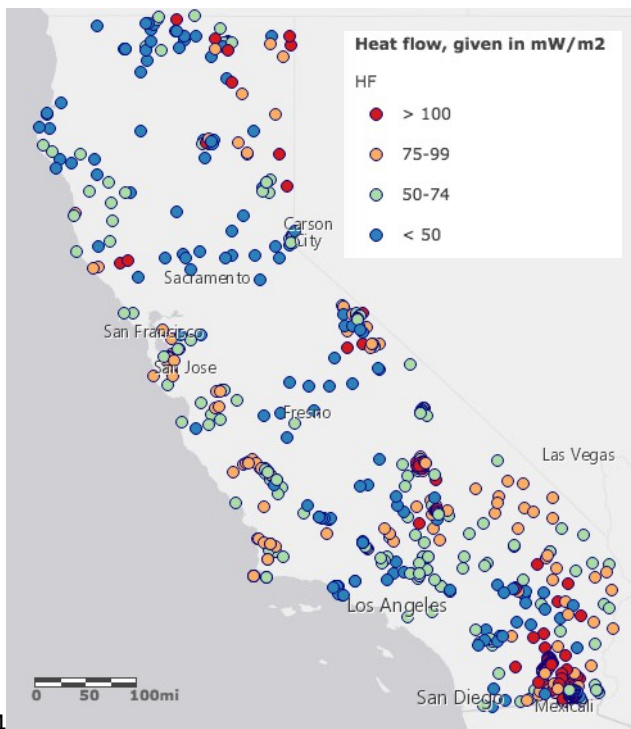
127An abandoned well is defined as a well with permanently discontinued use (NPC 2011). Well-
128plugging is a common practice which mitigates the hazards associated with unplugged
129abandoned wells, such as ground water contamination, ground water comingling, loss of aquifer
130pressure head, and uncontrolled gas migration (NDSU 2011). Specific plugging guidelines
131depend on formation consolidation magnitude, water table level, and oil presence. Newer
132plugging regulations call for a combination of sand, clay, and neat cement grouts to be shoveled
133into the well to create an impermeable plug in the well. California plugging regulations require a
13415 m long cement plug at the surface, cement plugs extending 30 m above oil bearing strata, and
135cement extending 15 m above and below water bearing strata (State of California 2007). Older
136wells (1850s spud dates) may have been plugged with brush, wood, rocks, paper, etc. according
137to loose regulations (Ide et al. 2006). Old or new, the cement plugs can be easily removed by
138setting up a special drill rig that breaks up and removes the well cement/debris (pers. comm., J.
139Trusche 2016).

1402.1 Crustal heat flow

141Crustal heat flow of California is well documented by numerous studies as shown in Figure 1
142(DeAngelo et al. 2013). The highest crustal heat flows are associated with geothermal anomalies
143south in Imperial County (Salton Sea, >100 mW/m², Combs 1971; Lachenbruch 1980), up north
144in Sonoma (Geysers, ~300 mW/m², Walters 1991), and central east California in Inyo County
145(Coso, >100 mW/m²). Heat sources for the Geysers, Coso and the Salton Sea geothermal power
146plants are magma chambers located at approximately 8 km depth (Nakamura 1980; Walters
1471991). Generally, the horizontal extent of the geothermal anomalies is <5 km (Nakamura 1980),
148so well temperatures in the observed regions are governed by crustal heat flow unless they drill
149into an anomaly. Figure 1 shows moderately high crustal heat flows along the coast in Santa

150Clara, South Monterey, and North Santa Barbara Counties (avg=84 mW/m², Walters 1991).
 151Inland, Lachenbruch et al. (1985) reported scattered locations of heat flows >100 mW/m² in San
 152Bernardino County.

153 Many of Imperial County's abandoned wells are focused on geothermal exploration south of
 154the Salton Sea largely due to the exceptionally high subsurface thermal gradients and the
 155presence of hydrothermal anomalies. Sass et al. (1984) reported thermal gradients ranging from
 1565.5-8.2 °C/100 m for shallow depths (<300 m). One abandoned well report shows a fluctuating
 157thermal gradient reaching as high as 18.2 °C/100 m and a bottom hole temperature of 220 °C at
 1582440 m (DOGGR, 2016). Similar to Imperial County, both the Geysers and Coso geothermal
 159fields also exhibit temperatures greater than 200 °C. However, the low number of abandoned oil
 160and gas wells in the proximity of the Geysers, Coso, and Imperial county removes them from the
 161interest of this paper, but it should be noted that any abandoned well (geothermal or oil/gas) in
 162these areas may be equally viable for well reuse given the bottom hole temperature remains >40
 163°C.



164
 165

166 **Figure 1.** Crustal heat flow map of California (created using publically available data and
 167 arcgis.com) (DeAngelo et al. 2013) (left) and California Geology and counties of interest
 168 (created using publically available geological map of California) (CGS 2016) (right)

169
 170 Santa Clara (and neighboring counties San Mateo and Santa Cruz), South Monterey, and
 171 North Santa Barbara are coastal regions characterized by medium to high heat flows and
 172 countless abandoned oil and gas wells (Table 2). Sass et al. (1971; 1994) measured several
 173 shallow less than 300 m deep thermal gradients in Sunnyvale, Santa Clara and reported an
 174 average thermal gradient of 5.8 °C/100 m. The thermal gradient may even reach higher values
 175 due to insulating lithological sequences, but assuming the thermal gradient stays constant at 5.8
 176 °C/100 m, a 1,220 m deep well in Santa Clara county should encounter 70 °C rock. Further
 177 deepening of the well’s depth by 1,000 m promises 130 °C rock. South in Monterey County,
 178 thermal gradients reported by the SAFOD down hole observatory reach 4 °C/100 m with a
 179 bottom hole temperature of 93 °C at 2,130 m (Williams et al. 2004). Further south, in the north
 180 region of Santa Barbara county, thermal gradients were reported as 4.9 °C/100 m with a bottom
 181 hole temperature of 60 °C at 1,220 m depth as shown in Figure 2 (Williams 1995). A rare
 182 temperature survey performed on an abandoned well in Santa Barbara reported a high thermal
 183 gradient of 7.3 °C/100 m with a bottom hole temperature of 55 °C at 670 m depth (DOGGR
 184 2016). Although the available temperature surveys are subject to error given the variety of
 185 methods used, abandoned wells in any of the coastal counties may provide access to crustal
 186 temperatures ranging from 48 to 93 °C without further well deepening. Methods of deepening the
 187 existing wells by 1000 m have a good chance of reaching rock temperatures, which can be
 188 candidates for electrical energy production.

189
 190 **Table 2. Comparison of abandoned well characteristics in California counties**

County	# Unused Wells ⁴	Max well depth/ (average) (m) ⁴	Temp Gradient (°C /100m)	Heat Flow ⁵ (mW/m ²)	Rock type at 2 km (deepest well) ⁴	Rock type at max depth (deepest well) ⁴
Santa Clara	5,184	2,000/(550)	5.8 (avg) ¹	75-99	Sandstone poor cons.	Sandstone poor cons.

Monterey	2,627	2,900/(700)	4.0 ²	75-99	Chert well cons. or granodiorite	Sandstone mod. cons or granodiorite
Santa Barbara	6,496	3,900/(770)	4.9 ³ - 7.3 ⁴	75-99	Claystone mod. cons.	Shale well cons.
Kern	81,000	6,600/(720)	2.0 ⁷ - 3.6 ⁴	50-75	Shale mod. cons.	Sandstone mod cons.
Fresno	8,435	4,900/(1,120)	2.5 ⁷	50-75	Siltstone poor to mod. cons.	Igneous volcanic poor cons.
Los Angeles	2,380	4,250/(1,800)	2.7 ⁴ - 5.5 ⁶	50-75	Shale well cons.	Sandstone well cons.
Ventura	8,364	5,000/(1,580)	2.2 ⁴ - 3.5 ⁶	50-75	Sandstone and shale poor to mod. cons.	Sandstone well cons.

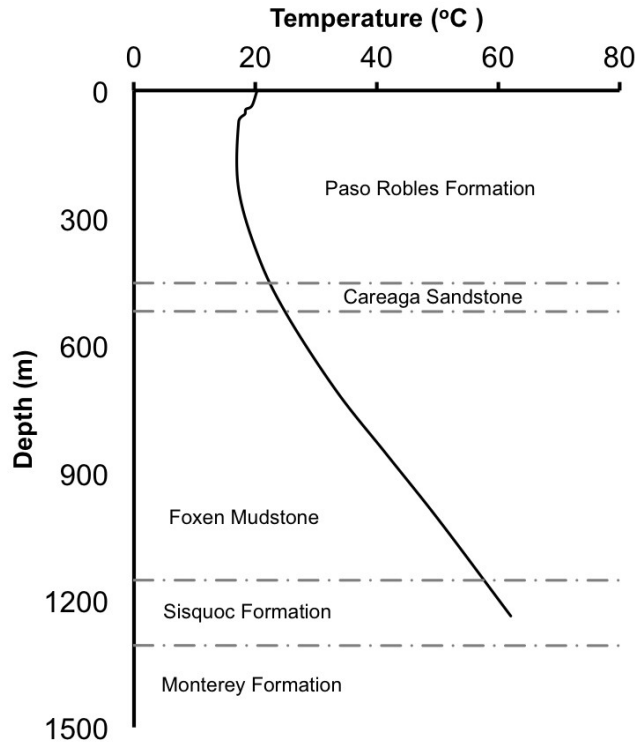
191 ¹Sass et al. 1994; ²Williams et al. 2004; ³Williams 1995; ⁴DOGGR 2016; ⁵DeAngelo et al. 2013; ⁶Higgins 1981;
192⁷Darton 1920

193

194 The previously mentioned counties were characterized by medium to high crustal heat flows,
195but other California counties still host vast numbers of abandoned wells and low-medium heat
196flows (50 to 75 mW/m²) as shown in Table 2. Such counties include Kern, Ventura, Fresno, and
197Los Angeles. A temperature survey on an abandoned well in Kern County measured a promising
198temperature gradient of 3.6 °C/100 m (DOGGR 2016). Another temperature survey on an
199abandoned well in Ventura County reported a gradient of 2.2 °C/100 m but a high bottom hole
200temp of 49 °C at 960 m (DOGGR 2016), possibly due to insulating rock layers. However,
201Higgins 1981 reported average gradients between 3.0 to 3.5 °C/100 m in the Ventura Basin. Los
202Angeles temperature gradients might be as low as 2.7 °C/100 m above 300 m, followed by a
203negative temperature gradient due to the presence of fluid (DOGGR 2016). In some isolated

204cases in the Palos Verdes basin of Los Angeles county, subsurface temperature gradients might
 205reach favorable values of 5.5 °C/100 m (Higgins 1981). Perhaps the reuse of wells in the Palos
 206Verdes basin of Los Angeles county counties is less viable, but the abandoned wells may be
 207candidates for well deepening if the local geology is conducive to geothermal fluid circulation
 208and the surface industrial application is justified for the area.

209



210

211 **Figure 2.** Thermal gradient and lithology for a well located in Santa Maria (North Santa Barbara
 212 County) (Williams 1994) (sized for single column)

213

214 **2.2 Geology**

215 Another important characteristic of EGS is the geology of the geo-reservoir. Rock permeability
 216 must be low enough to maintain working fluid pressure (i.e. avoid fluid loss), but it also must be
 217 high enough for the working fluid to migrate through the rock quickly enough to maintain
 218 required flow rates (Tester et al. 2006). Existing pilot EGS sites target igneous rock formations,
 219 such as granite, where fluid circulation through hot crystalline rock mass relies on stimulated
 220 permeability by means of hydraulic fracturing or shear displacement of the existing fracture
 221 network. Although sandstone and other sedimentary rocks cannot support the same type of

222fracture network due to higher permeability, some studies have demonstrated the capacity of
223sandstone to support high flow rates and minimal fluid loss. For example, sandstone’s natural
224primary porosity was combined with stimulated secondary porosity to establish a geothermal
225reservoir (Legarth et al. 2005; Bolcher et al. 2009; and Zimmerman et al. 2010). Zimmerman et
226al. (2010) employed a gel proppant stimulation in a 1250 m deep sandstone formation
227characterized by 8-10% porosity, 150 °C and 16.5 mD permeability underlain by a low
228permeability igneous rock layer. The study concluded that the sustainability of the sandstone
229fractures was key to the success of the sandstone reservoir. Additional evidence pointing toward
230the suitability of sandstone for EGS is the occurrence of natural hydrothermal anomalies in
231sandstone formations and granitic plutons alike (Loucks and Milliken 1981). Therefore, EGS
232may be suitable in formations comprised of sandstone layers characterized by lower porosities
233and lower permeability “caps” to control fluid migration.

234 Most of the abandoned wells in California target oil and gas rich sandstones and shales. Thus,
235these wells tend to drill through and into marine sedimentary rocks. The geology of Santa Clara
236County varies from moderately consolidated to loosely consolidated marine and non-marine
237sedimentary rocks (Figure 1, CGS 2016). Mud logs for abandoned wells show lithology
238(including San Jose) comprised of mostly silty and sandy shales down to 1,000 m (DOGGR
2392016). One well closer to the coast shows 460 m of shale covering a 90 m thick layer of “Costa
240Sandstone” at 850 m depth. Indirect neutron porosity measurements estimate true formation
241porosity around 10-25% at these depths (DOGGR 2016). South of Santa Clara, the geology of
242Monterey is similar but comprised of more frequent alternating sequences of sandstone, shale,
243and siltstone. CGS (2016) reports the geology as loosely to moderately consolidated alluviums.
244These sandstone layers range from 15 to 60 m thick with porosity values hovering around 10 to
24515% (DOGGR 2016). One unique feature of the Monterey County geology is the presence of a
246granodiorite floor around 700 m depth for wells further than 5 km from the San Andreas fault
247(DOGGR 2016). South of Monterey County in Santa Barbara, the geology is reported as the
248same coastal alluvial deposits with low to moderate consolidation (Figure 1). Various wells in the
249region report mostly alternating 15 to 60 m thick layers of clay and shale. However, a notable
250geological shift to sandstone occurs at about 850 m depth as shown in Figure 2 (DOGGR 2016).
251Although many mud log records do not report rock types beyond 1,000 m depth, the alternating
252sequences of sedimentary rock described above can be assumed to continue until basement,

253which exists at depths between 4,000 and 10,000 m (Higgins 1981). Table 2 shows the rock
254formations encountered at 2,000 m depth and at the max depth reached for the deepest well in
255each county.

256 The geology of inland oil fields in regions characterized by lower heat flows is similar to
257coastal California geology (Figure 1). The majority of wells comprising the Ventura oil and gas
258field drill into moderately consolidated marine sedimentary rocks from the Pliocene period. For
259example, a representative well might hit oil-bearing shale at 2000 m followed by hard sandstone
260at 2050 m followed by shale with streaks of sand at 2057 m. Around 2285 m the wells hit
261variations of hard shale containing oil, gas, or sand (DOGGR 2016). Fresno County wells reach
262unconsolidated or semi-consolidated non-marine alluvium deposits. The Southern Fresno and
263Kern County wells describe alternating claystone, blue shale, siltstone, and poorly sorted
264sandstone down to 1370 m (DOGGR 2016). Wells logged for density show porosity hovering
265around 15% between 1370 and 2130 m (DOGGR 2016). A well near the middle of Fresno
266County offers lithology to a depth of 3000 m. On the way down clay confines 30 to 60 m thick
267layers of very fine grained sands. At 3000 m a granitic floor marks a geologic transition. A
268similar geology is observed in the Palos Verdes basin of Los Angeles County where 1,500 to
2694,000 m of Cenozoic marine sediments overlie crystalline basement (Higgins 1981).

270 Finally, the geology of Imperial County shares a similar geology to Fresno County: marine
271and non-marine unconsolidated/semi consolidated alluvial sedimentary deposits comprising part
272of the Palm Springs Formation (CGS 2016). Mud logs show alternating lithology of 15 to 30 m
273thick layers of sandstone and claystone. Formation porosity was measured at 15% around 1250
274m depth (DOGGR 2016). The aforementioned well was drilled in 1978, but due to an apparent
275lack of water productivity the well was plugged and abandoned in 1987. An active liquid
276dominated geothermal well field (East Mesa) in Southeast Imperial County accesses 120 to 150
277°C fluids in sandstone covered by shale caprock (DOGGR 2016). Some wells nearby this field
278access high temperatures and great depths (96 °C at 2,040 m, DOGGR, 2016) but were plugged,
279presumably because they produced little or no fluid. Sass et al. (1984) measured shallow
280porosities in the area ranging from 15 to 40%.

281 To conclude, the coastal and inland lithology of California may prove suitable for EGS,
282especially the geological setting in Monterey. Monterey's low porosity sandstone formation
283underlain by a shallow granodiorite basement in combination with a medium to high heat flow

284might enable a similar EGS configuration to that of Zimmerman et al. (2010). The Zimmerman
285et al. (2010) project used hydraulic fractures extending from a crystalline basement up into the
286overlying sandstone formation to deliver water to the sandstone formation where the water
287permeated the sandstone before reaching a production well. Other counties also sit on crystalline
288basements, but these basements range from 4,000 to 10,000 m depth (Higgins 1981) and need to
289be further evaluated.

2902.3 Stress regimes

291The development of EGS involves the stimulation of formation porosity by means of hydraulic
292fracturing or hydroshearing. Since fracture propagation is governed by in-situ stress direction
293and magnitudes, the crustal stress state is reported here for each of the regions of interest to
294illustrate in-situ EGS suitability. The general stress setting is strike-slip, demonstrated by the
295proximity of these counties to the San Andreas Fault. However, local stresses may be rotated due
296to the weak shear strength of the fault and historically active stresses in the region (Zoback et al.
2971987). The conclusions suggest a normal/strike-slip stress regime, both of which encourage
298vertically oriented fracture planes. SAFOD provides insight into the stress state at great depths in
299Monterey and other regions along the San Andreas Fault. Borehole breakouts and drilling
300induced tensile fractures were used to constrain a transitional strike-slip to reverse faulting
301regime (Hickman and Zoback 2004). This conclusion suggests the possibility of compressional
302horizontal confinement stresses being larger than the compressional vertical confinement stress,
303which may yield horizontal fracture plane orientations. Hardebeck and Hauksson (2001) used
304earthquake focal mechanisms to estimate the stress orientation of Southern California. Findings
305show that Los Angeles follows a similar transitional regime of strike-slip to reverse, while down
306south in Imperial County the regime follows a transitional normal to strike-slip faulting pattern.

3073. PERMEABILITY STIMULATION OF SEDIMENTARY ROCK FORMATIONS

308The implementation of an EGS system in abandoned oil and gas wells in California depends
309strongly on the hydraulic fracturing processes within loosely to moderately consolidated
310sedimentary rock. The Geothermal Reservoir Well Stimulation Program in the USA showed that
311Hydraulic Proppant Fracturing (HPF) can be applied to sedimentary formations (Campbell et al.
3121981; Entingh 2000). Specific to California's sandstone geology, the sandstone siltstone rock
313matrix of the East Mesa geothermal site experienced an apparent increase of permeability
314following HPF treatment, which corresponded to a doubled production flow rate (Campbell et al.

3151981: Entingh 2000). One of the East Mesa HPF treatments was performed at 1500 m depth and
316successfully corrected permeability impairment near the wellbore. Although East Mesa is a
317hydrothermal system, the HPF treatment is of specific relevance to the current study due to the
318common geology, abandoned well depth (1500 m), and management of near wellbore damage.

319 Despite reported successful sandstone HPF treatments, Legarth et al. 2005 outlines
320difficulties encountered in the poorly cemented Rotliegend sandstone. Particularly, the
321unforeseen mechanical and chemical processes occurred during the fracture closure. Zimmerman
322et al. 2011, however, details the successful permeability enhancement of the same Rotliegend
323sandstone by application of a revised gel-proppant treatment. The treatment involved the
324injection of resin coated high strength proppant in high viscosity cross-linked gel. Both studies
325indicate the importance of better understanding the fracture stimulation design, fracture
326propagation associated with flow rates, treatment duration, and fluid dynamic viscosity.

327 The prediction of fracture propagation and the applicability of the Linear Elastic Fracture
328Mechanics (LEFM) to the loosely to moderately consolidated sandstone is still not well
329understood. Khodaverdian and McElfresh (2000) experimentally observed both the pore pressure
330increase and the development of high shear stress within the process zone at the fracture tip due
331to the plasticity of loosely consolidated sandstone. The observations by Khodaverdian and
332McElfresh (2000) pointed toward a shear failure within the plastic zone unexplained by LEFM
333and largely controlled by pore pressure increase in the process zone ahead of the fracture tip.
334Bohloli and De Pater (2006) demonstrated that the viscosity of the injected fluid has as much
335control over the geometry and extent of fractures in loosely consolidated rock, as the injected
336fluid pressure. Despite these challenges, advances in numerical modeling (Zhai and Sharma
3372005) coupled with decades of directional drilling and hydraulic fracturing of sandstones (Monus
338et al. 1992) provide a strong foundation for the development of EGS in loosely to moderately
339consolidated sandstone formations.

3404. LOW TEMPERATURE HEAT EXTRACTION BY DEEP BHE FEASIBILITY STUDY

341The feasibility of reusing abandoned oil and gas wells as deep BHEs is investigated by
342mathematically modeling fluid flow through a coaxial deep BHE configuration. Convective and
343conductive heat transfer are modeled between the incompressible fluid and the surrounding rock
344matrix. An envelope of desirable crustal temperature gradients, well depths, and flow rates is

345determined by parameterizing the deep BHE model according to well and heat flow
 346characteristics observed in Santa Barbara, Santa Clara, and Monterey, California, USA.

3474.2 Methodology

348The numerical solutions to the equations for fluid flow and heat transport are solved using the
 349finite element method in COMSOL Multiphysics software. The governing equations for the
 350model include Navier-Stokes for fluid flow through the BHE and conservation of energy for
 351convective and conductive heat transfer. The fluid is assumed incompressible ($\nabla \cdot u = 0$) and
 352the inertial forces are assumed to be much smaller than viscous forces. Thus, the Navier-Stokes
 353equation is reduced to:

354

$$0 = -\nabla p + \nabla \cdot (\mu (\nabla u + (\nabla u)^T)) \quad (1)$$

355

356where p is the fluid pressure (Pa), u is the fluid velocity (m s^{-1}), and μ is the fluid
 357dynamic viscosity ($\text{Pa}\cdot\text{s}$). For convective and conductive heat transfer, the conservation of energy
 358equation can be written as:

359

$$\rho C_p u \cdot \nabla T = \nabla \cdot (k \nabla T) + Q_c \quad (2)$$

360

361where ρ is the water density (kg m^{-3}), C_p is the water specific heat capacity ($\text{J kg}^{-1}\text{K}^{-1}$), T
 362is the temperature (K), Q_c is a heat source (crustal heat flow) (W m^{-2}), and k is the thermal
 363conductivity of rock or water (W(mK)^{-1}). The term on the left-hand side of Eq. 2 describes the
 364heat convection associated with the fluid flow. The current study investigates long-term
 365industrial applications for deep BHEs. Therefore, the equations are solved for the steady-state
 366since BHE production temperatures fall with time and ultimately plateau (Aachen, Germany -
 367Dijkshoorn et al., 2013).

368 This study uses the Coefficient of Performance (COP) as a metric for comparing
 369parameter combinations.

370

$$COP = \frac{Q_r}{W_p} \quad (3)$$

$$Q = C_p \rho q (T_{out} - T_{in}) \quad (4)$$

371

372 where Q_r is the thermal heat extracted from the reservoir (W), C_p is the heat capacity of
 373 water ($\text{J kg}^{-1}\text{K}^{-1}$), ρ is the density of water (kg m^{-3}), q is the fluid flow rate through the
 374 BHE, T_{out} and T_i are the inlet and outlet fluid temperatures of the coaxial BHE (K), and
 375 W_p is the work consumed by the electrical water pump (W):

376

$$W_p = \frac{q \rho g h_f}{\eta} \quad (5)$$

377

378 where g is the acceleration due to gravity (m s^{-2}), η is the pump efficiency (0.8), and
 379 h_f is the headloss due to friction (m) as defined by the Darcy-Weisbach equation:

380

$$h_f = f_D \frac{L V^2}{D 2g} \quad (6)$$

381

382 where L is the length of the heat exchanger (m), V is the velocity of the fluid, D is the
 383 hydraulic radius of the pipe (m), and f_D is the friction factor defined by using the Reynolds
 384 number (Re):

385

$$\Re = \frac{\rho V D}{\mu} \quad (7)$$

386

387 and relative pipe roughness, ε/D , (ε is 0.025 for steel) with the Moody diagram.

388 The heat transfer across the inner and outer well casings was computed using a pair thin
 389 layer resistive layer boundary condition:

390

$$q_2 = \frac{T_1 - T_2}{d_s / k_s} \quad (8)$$

391

392 where T_1 is the temperature on the inside of the layer and T_2 is the temperature on the
 393 outside of the layer, d_s is the thickness of the thin layer (m), k_s is the thermal conductivity
 394 of the thin layer (W(mK)^{-1}), and q_2 is the heat flux vector on the outside of the layer (W m^{-2}).

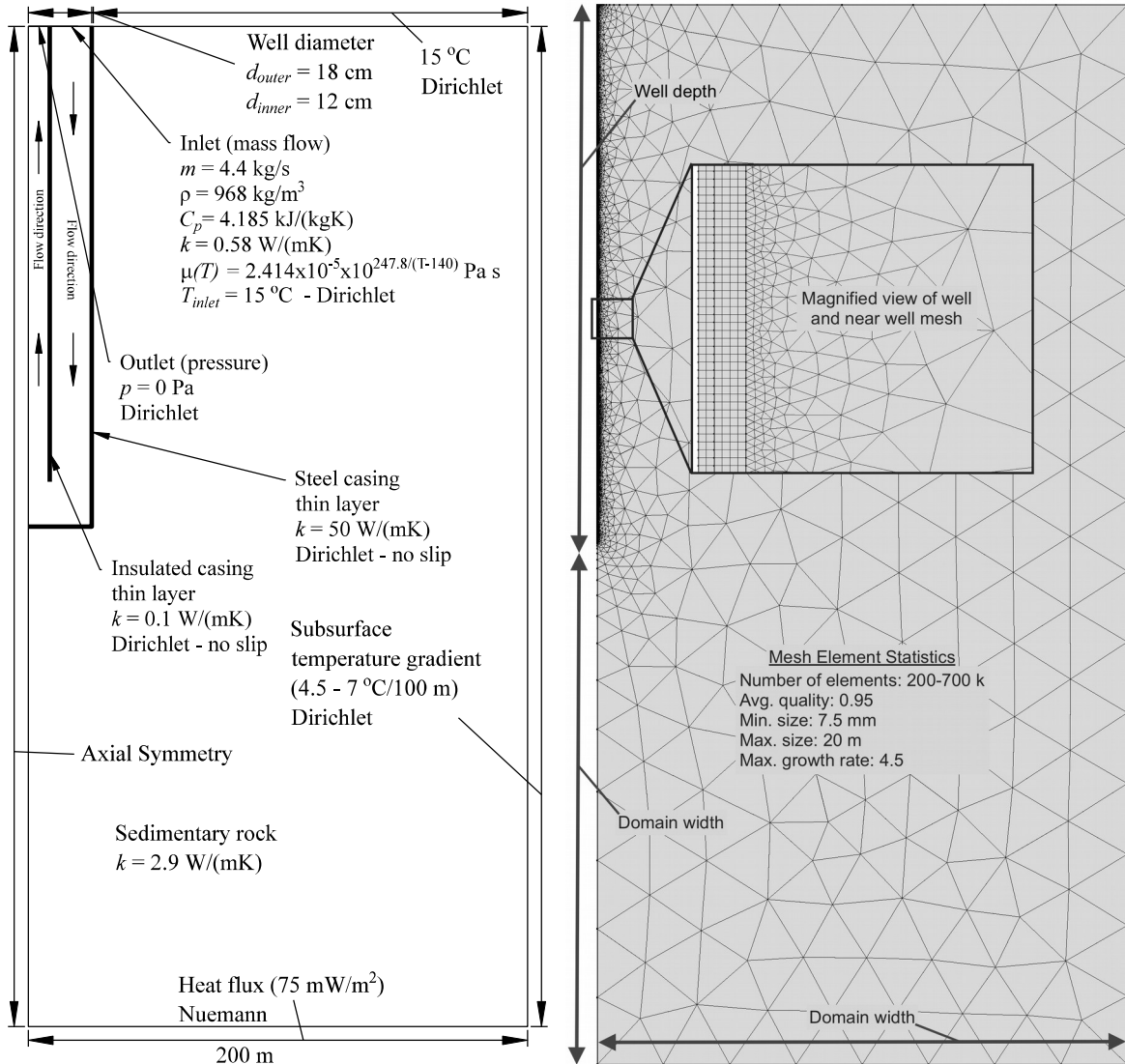
395 q_1 is simply the opposite of q_2 .

396 Well and reservoir model domain geometry and mesh are shown in Figure 3. The
397 domains are discretized in 2D and the final solution is axisymmetric. The modeled well depths
398 are 1000, 3000 and 5000 m, which match well depths encountered in Santa Barbara, Santa Clara,
399 and Monterey county. The 200 m width of the domain was determined by convergence study
400 shown in Figure 4 to provide a sufficient buffer between the boundary conditions and the well
401 domain. Beyond 200 m domain width, the steady state outlet temperature remains unaffected.
402 The coaxial BHE configuration dimensions follow the dimensions of existing abandoned wells
403 of interest: 180 mm and 120 mm outer and inner diameters, respectively. Figure 3 shows the
404 FEM discretization of the domains, where the element size ranges from 7.5 mm in the well to 20
405 m at the boundary of the domain.

406 Model boundary and initial conditions are shown in Figure 3. The edge of the model
407 follows a variable-with-depth temperature boundary condition (Dirichlet) to simulate crustal
408 temperature gradient. Values for the edge boundary conditions were parameterized to 4.5 and 7.0
409 °C/100m, which match the range observed in Santa Barbara, Santa Clara, and Monterey. The
410 bottom of the domain was constrained by a constant heat flux of 75 mWm⁻² (Nuemann) boundary
411 condition, which follows crustal heat flow estimates gathered by several geological surveys
412 (DeAngelo et al. 2013) for the counties of interest. The inlet mass flow rate of the coaxial heat
413 exchanger was parameterized to 1, 4.4, and 10 kg/s, which aligns with the heating demand of a
414 single commercial building (Dijkshoorn et al. 2013). For the outlet of the coaxial heat exchanger,
415 a constant pressure boundary condition of 0 Pa was used. The boundary condition of the fluid
416 flow domain (well casing) is no-slip (velocity of fluid at wall is 0 m/s).

417 In summary, a total of 18 parameter combinations are used for this study. Specifically,
418 well depths of 1000, 3000, 5000 m, mass flow rates of 1, 4.4, 10 kg s⁻¹, and edge temperature
419 gradients of 4.5 and 7.0 °C/100m.

420



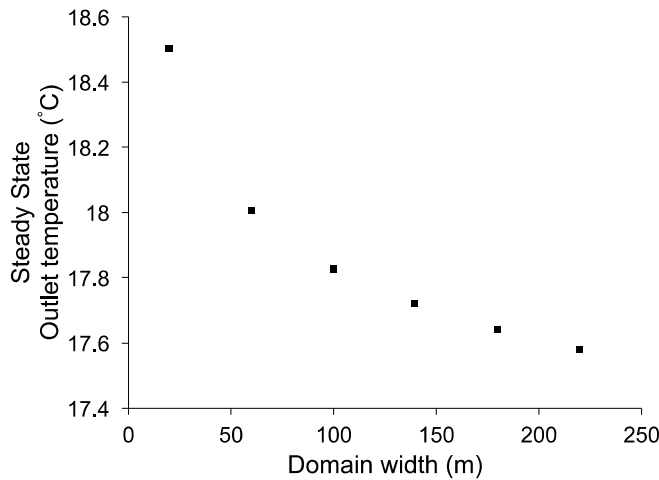
421

422 **Figure 3.** Model geometry and details (not to scale) (left) and domain discretization (right)

423

424 Model parameters are also reported in Figure 3. Effective thermal conductivity, k , was used
 425 to represent the sedimentary rock surrounding abandoned wells in California. Saturated
 426 sandstones with average quartz content and porosities ca. 10 to 15% exhibit effective k as
 427 high as 4.5 W/(mK)⁻¹ while unsaturated shales exhibit lower effective k closer to 1.25 W/(mK)⁻¹
 428¹ (Robertson 1988). For these reasons an average effective k of 2.9 W/(mK)⁻¹ is used to
 429 represent the semi saturated sandstones encountered in the counties of interest. The model uses a

430thermal conductivity of 0.1 W(mK)^{-1} for the insulating inner pipe, which matches the installed



431

432

Figure 4. Domain width convergence study

433

434 conductivity of the double-walled vacuumed insulating pipe the deep BHE of Weggis
435Switzerland (Kohl et al. 2002).

436

4374.3 Results

438This feasibility study estimates the production temperatures and flow rates for abandoned wells
439converted to deep BHEs in Santa Barbara, Santa Clara, and Monterey counties. Various depths
440(1000 to 5000 m), temperature gradients (4.5 to $7.0 \text{ }^\circ\text{C}/100 \text{ m}$), and flow rates (1 to 10 l/s) result
441in a wide range of fluid temperature increases between 1.2 and $130 \text{ }^\circ\text{C}$. Figure 5 shows how
442lower flow rates (1 l/s) are necessary to achieve fluid temperature increases $>10 \text{ }^\circ\text{C}$ in 1000 m
443deep wells. However, in deeper wells (ca. 3000 m) the temperature gradient plays a larger role in
444increasing the outlet fluid temperature beyond the target for direct use. An increased subsurface
445gradient from 4.5 to $7 \text{ }^\circ\text{C}/100 \text{ m}$ increased the production temperature by 36.5 % for 4.4 l/s flow
446rate in a 3000 m deep well. Flow rate also plays a key role, a change of flow rate from 1 to 10 l/s
447decreases the production fluid temperature by 40.7 % for a 3000 m deep well characterized by 7
448 $^\circ\text{C}/100 \text{ m}$. Figure 5 also shows how the impacts of subsurface temperature gradient and flow rate

35

18

36

449 become greater as well depth increases. Ultimately, the target well depth, flow rate, and
 450 subsurface temperature gradients range from 1250 m with 1 l/s flow rate and 7 °C/100 m to 5000
 451 m with a flow rate of 10 l/s and 4.5 °C/100 m.

452 The COPs for the analyzed combinations of fluid flow rates, well depths and subsurface
 453 temperature gradients are shown in Figure 6. It is observed that COP increases with well depth
 454 and decreases with increasing flow rate. The COP for the flow rate of 4.4 l/s increases by ca.
 455 425% with well depth between 1000 and 5000 m and decreases for a 3000 m deep well by ca.
 456 50% as flow rate increases from 4.4 to 10 l/s. Although the general trend follows an increasing
 457 COP with increasing well depth, at low flow rates and high well depths the COP starts to decline.
 458 This decline is caused by the low Reynolds number which corresponds to a higher friction factor

459 ($f_D \dot{v}$ from the Moody diagram leading to increased head loss due to friction $\frac{h}{L} \dot{v}$, Eq. 6) and
 460 the work necessary to pump the fluid (W_p , Eq.5), yielding a lower COP (Eq. 3)

461 A similar analysis was run by Śliwa et al. 2015, however that analysis focused on well
 462 coaxial configurations. Table 3 shows the comparison of two similar simulations. Despite
 463 differing insulation thermal conductivity and flow rates, the similarity of the results validates the
 464 methods used in both studies.

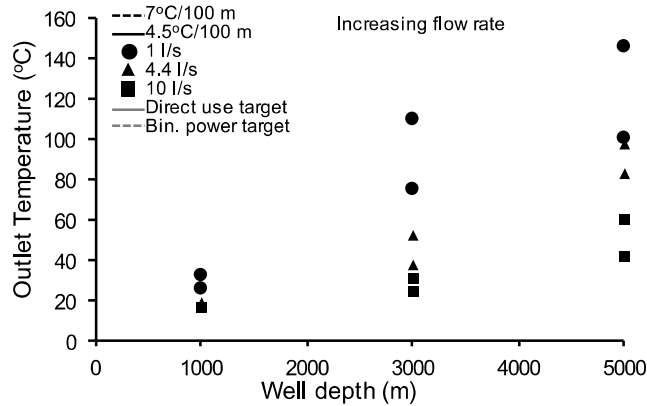
465

466 **Table 3.** Deep BHE simulation comparison

	Śliwa et al. 2015	Present study
Well depth (m)	2316	1600
Bottom hole temp (°C)	73.5	72
Flow rate (l/s)	2.5	4.4
Inlet temperature (°C)	11.6	15
Insulating thermal conductivity (Wm ⁻¹ K ⁻¹)	0.26	0.1
Outlet temperature (°C)	23	ca. 25
Well diameter (outer, inner mm)	120, 70	180, 120

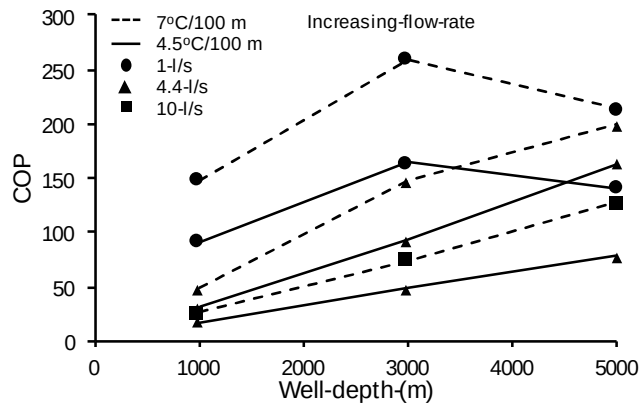
467

468



469

470 **Figure 5.** Steady-state coaxial BHE outlet fluid temperature for various flow rates, well depths,
 471 and subsurface temperature gradients



472

473 **Figure 6.** COP for various flow rates, well depths, and subsurface temperature gradients

474

4755. **CONCLUSIONS**

476 The vast number of abandoned wells in California presents an opportunity for the development
 477 of low cost renewable geothermal energy. This paper identified counties within California
 478 characterized by a high number of abandoned oil and gas wells, medium to high crustal heat
 479 flows, and sedimentary geology suitable for the extraction and direct use of geothermal energy
 480 via sedimentary EGS and deep BHE. These counties include Santa Clara, Monterey, and Santa
 481 Barbara, and they may benefit from a local investigation of abandoned wells to better understand
 482 their suitability for a low temperature direct use. For example, district heating requires a close
 483 proximity to users, while industrial applications such as greenhouses or aquaculture need to be
 484 located at the abandoned well site.

485 In general, the abandoned wells located in Santa Clara, Monterey, and Santa Barbara counties
 486 tap into low to moderately consolidated sandstone rock layers at depths of 900 to 2000 m

487 confined by shale layers with similar consolidation characteristics. Bottom hole temperatures
488 depend strongly on crustal heat flow and well depth, but in general temperatures range from 40
489 to 70 °C with some wells reaching up to 90 °C. These depths and temperatures are suitable for
490 direct use low temperature EGS such as district heating or greenhouse heating. The paper
491 identified other counties characterized by high numbers of abandoned wells and suitable
492 sedimentary geology, but low crustal heat flow. These counties include Fresno, Kern, Ventura,
493 and Los Angeles. The abandoned wells within these counties exhibit temperature gradients as
494 low as 2.2 °C/100 m and may require deepening of several hundred meters to reach usable
495 temperatures.

496 Although the bottom well temperatures in Santa Clara, Monterey, and Santa Barbara are
497 already suitable for EGS, one of the challenging issues is the prediction of hydraulic fractures in
498 loosely to moderately consolidated sedimentary rock for various stress regimes. In some cases, it
499 may be desirable to identify regions characterized by reverse faulting regimes depending on the
500 proposed abandoned well reuse. A single well EGS may benefit greater from a reverse faulting
501 regime that would enable several individually stimulated horizontal fracture zones stacked
502 vertically. This configuration allows operators to pump water into one zone, and produce hot
503 water from another zone, all within the same well. In other cases, the normal or strike-slip
504 regime may suit a double well system better since the control of water migration is easier with
505 vertical fractures and vertical wells. However, directional drilling enables regime controlled well
506 configurations (i.e. within a strike-slip faulting regime, a well could be directionally drilled to
507 enable a single well EGS). Despite the versatile nature of EGS, experimental and numerical
508 research still needs to be conducted to better understand the mechanics of hydraulic fracturing in
509 the specific rock types found in the aforementioned California counties. Further, models should
510 incorporate transitional stress regimes for better predicting the path of hydraulic fractures.

511 Deep coaxial BHE is a feasible low cost, low-risk alternative to EGS. Results of a
512 mathematical model conclude that target outlet temperatures >40 °C are easily achievable for
513 counties with high temperature gradients (7 °C/100 m). A 180 mm diameter coaxial BHE yields
514 >40 °C production temperatures for well depths >1250 m and flow rates between 1.0 to 4.4 l/s (it
515 should be noted that 40 °C can also be achieved with 10.0 l/s and a 4000 m deep well). The
516 results of the deep BHE simulation also indicate that flow rate negatively impacts the COP while
517 well depth improves the COP for moderate to high flow rates. Findings show that despite high

518 production temperatures at low flow rates, the COP is larger for moderate flow rates (4.4 l/s) and
519 great depths (5000 m). Flow rates between 0.8 and 6.0 l/s are currently used in deep BHEs for
520 district heating in various buildings throughout Europe.

521 The study found that deep BHE is suitable for counties with high and low heat flows. Santa
522 Barbara is characterized by high temperature gradients and high numbers of deep abandoned
523 wells. These depths and temperatures could support a variety of industrial low-temperature
524 applications such as greenhouses, water desalination, and general space heating. In counties
525 characterized by lower temperature gradients ($<4.5\text{ }^{\circ}\text{C}/100\text{ m}$), $40\text{ }^{\circ}\text{C}$ water temperatures can
526 only be achieved with well depths of 3000 to 5000 m. Fortunately, the counties characterized by
527 lower temperature gradients (Kern, Fresno, Los Angeles, Ventura) also host substantial numbers
528 of abandoned wells deeper than 3000 m, making them suitable for deep coaxial BHE
529 investigations. It is worth noting that lower production temperatures ($<40\text{ }^{\circ}\text{C}$) associated with
530 shallower wells ($<1000\text{ m}$) and lower temperature gradients ($<4.5\text{ }^{\circ}\text{C}/100\text{ m}$) can also be coupled
531 with a heat pump to deliver viable fluid temperatures for general space heating. Although the
532 addition of a heat pump would reduce efficiency, a solar power coupling could offset the energy
533 costs and pair well with unique direct geothermal uses such as greenhouse-water desalination
534 (Goosen et al. 2010) or a reverse osmosis desalination configuration (Houcine et al. 1999; Kamal
535 1997). Furthermore, less desirable geological conditions might produce exceptional heat
536 production if the thermal loading is cyclic instead of steady. For example, Kohl et al. 2002
537 observed $40\text{ }^{\circ}\text{C}$ production temperatures from a 2133 m deep $3.0\text{ }^{\circ}\text{C}/100\text{ m}$ BHE in Weggis,
538 Switzerland.

539 In conclusion, abandoned oil/gas wells in California may provide a starting point for well
540 deepening, but in other cases the abandoned wells may only require unplugging and re-casing to
541 isolate sandstone formations of interest (EGS) or increase casing contact with surrounding rock
542 (deep coaxial BHE). In all cases, a mitigation of drilling costs corresponds to a reduced EGS
543 project cost of 42%-95% (Tester et al., 1994).

544

545 REFERENCES

546 Bai, F., Akbarzadeh, A., Singh, R. (2010). "Combined Freshwater Production and Power
547 Generation from Geothermal Reservoirs." Proceedings World Geothermal Congress,
548 Bali, Indonesia, 25-29 April 2010.

549Bohlooli, B., & De Pater, C. J. (2006). "Experimental study on hydraulic fracturing of soft rocks:
550 Influence of fluid rheology and confining stress." *Journal of Petroleum Science and*
551 *Engineering*, 53(1), 1-12.

552Blocher, G., Zimmermann, G., & Milsch, H. (2009). Impact of poroelastic response of
553 sandstones on geothermal power production. *Pure and Applied Geophysics*, 166(5–7),
554 1107–1123. <http://doi.org/10.1007/s00024-009-0475-4>

555California Geological Survey (CGS). Department of Conservation. Geologic Map of California.
556 Available online at <http://maps.conservation.ca.gov/cgs/gmc/>. Accessed on June 10, 2016.

557Campbell, D., Morris, C., & Verity, R. (1981). Geothermal Well Stimulation Experiments and
558 Evaluation. *Proceedings of SPE Annual Technical Conference and Exhibition*, 10.
559 <http://doi.org/10.2118/10316-MS>

560Combs, Jim. (1971). "Heat flow and geothermal resource estimates for the Imperial Valley." *RW*
561 *Rex (Principal Investigator), Cooperative Geological-Geophysical-Geochemical*
562 *Investigations of Geothermal Resources in the Imperial Valley Area of California.*
563 *University of California, Riverside*: 5-27.

564Darton, N. H. (1920). *Geothermal data of the United States: including many original*
565 *determinations of underground temperature* (No. 697-701). Govt. Print. Off.

566DeAngelo, J., Galanis, S. P., Grubb, F., Palguta, J., Reed, M., Williams. C. (2013). California
567 Heat Flow Studies. USGS. Retrieved from
568 <http://geomaps.wr.usgs.gov/heatflow/index.htm> on June 10, 2016.

569Department of Conservation Division of Oil, Gas, and Geothermal Resources (DOGGR).
570 Department of Conservation. Well Search. Retrieved from
571 <https://secure.conservation.ca.gov/WellSearch/> on June 10, 2016.

572Dijkshoorn, L., Speer, S., & Pechnig, R. (2013). Measurements and design calculations for a
573 deep coaxial borehole heat exchanger in aachen, Germany.*International Journal of*
574 *Geophysics*, 2013.

575Economides, M.J. ed., (2000). *Reservoir stimulation* (Vol. 18). Chichester: Wiley.

576Goosen, M., Mahmoudi, H., & Ghaffour, N. (2010). Water Desalination using geothermal
577 energy. *Energies*, 3(8), 1423–1442. <http://doi.org/10.3390/en3081423>

578Hardebeck, J. L., & Hauksson, E. (2001). "Crustal stress field in southern California and its
579 implications for fault mechanics." *Journal of Geophysical Research B*, 106(B10), 21859-
580 21882.

581Hickman, S., & Zoback, M. (2004). "Stress orientations and magnitudes in the SAFOD pilot
582 hole." *Geophysical Research Letters*, 31(15).

583Higgins, C. T. (1981). *Reconnaissance of geothermal resources of Los Angeles County,*
584 *California* (No. DOE/SF/10855-3). California State Dept. of Conservation, Sacramento
585 (USA). Div. of Mines and Geology.

586Houcine, I., Benjemaa, F., Chahbani, M. H., & Maalej, M. (1999). Renewable energy sources for
587 water desalting in Tunisia. *Desalination*, 125(1), 123-132.

588Kamal, I. (1997). "Thermo-economic modeling of dual-purpose power/desalination plants: steam
589 cycles." *Desalination*, 114(3), 233-240.

590Khodaverdian, M., & McElfresh, P. (2000). "Hydraulic fracturing stimulation in poorly
591 consolidated sand: mechanisms and consequences." In *SPE Annual Technical Conference*
592 *and Exhibition*. Society of Petroleum Engineers

593Kohl, T., Brenni, R., & Eugster, W. (2002). "System performance of a deep borehole heat
594 exchanger." *Geothermics*, 31(6), 687-708.

595Kohl, T., Salton, M., & Rybach, L. (2000). "Data analysis of the deep borehole heat exchanger
596 plant Weissbad (Switzerland)." In *Proc. World Geothermal Congress* (pp. 3459-3464).

597Kulcar, B., Goricanec, D., & Kroppe, J. (2008). "Economy of exploiting heat from low-
598 temperature geothermal sources using a heat pump." *Energy and buildings*, 40(3), 323-
599 329.

600Lachenbruch, A. H., & Sass, J. H. (1980). "Heat flow and energetics of the San Andreas fault
601 zone." *Journal of Geophysical Research: Solid Earth*, 85(B11), 6185-6222.

602Lachenbruch, A. H., Sass, J. H., & Galanis, S. P. (1985). "Heat flow in southernmost California
603 and the origin of the Salton Trough." *Journal of Geophysical Research: Solid*
604 *Earth*, 90(B8), 6709-6736.

605Legarth, B., Huenges, E., & Zimmermann, G. (2005). "Hydraulic fracturing in a sedimentary
606 geothermal reservoir: Results and implications." *International Journal of Rock*
607 *Mechanics and Mining Sciences*, 42(7–8 SPEC. ISS.), 1028–1041.
608 <http://doi.org/10.1016/j.ijrmms.2005.05.014>

609Li, M., & Lior, N. (2014). “Comparative Analysis of Power Plant Options for Enhanced
610 Geothermal Systems (EGS).” *Energies*, 7(12), 8427–8445.
611 <http://doi.org/10.3390/en7128427>

612Loucks, R. G., Richmann, D. L., & Milliken, K. L. (1981). *Factors controlling reservoir quality*
613 *in Tertiary sandstones and their significance to geopressured geothermal production* (No.
614 DOE/ET/27111-T3). Texas Univ., Austin (US). Bureau of Economic Geology (US).

615Lund, J. W., & Lienau, P. J. (1997). “Geothermal district heating.” *Proceedings of International*
616 *Course on Geothermal District Heating Schemes, Çeşme, Izmir, Turkey,(19–25 October,*
617 *1997)*, 1-27.

618Lund, J. W., & Boyd, T. L. (2016). “Direct utilization of geothermal energy 2015 worldwide
619 review.” *Geothermics*, 60, 66-93.

620Monus, F. L., Broussard, F. W., Ayoub, J. A., & Norman, W. D. (1992). “Fracturing
621 unconsolidated sand formations offshore Gulf of Mexico.” In *SPE Annual Technical*
622 *Conference and Exhibition*. Society of Petroleum Engineers.

623Østergaard, P. A., & Lund, H. (2011). “A renewable energy system in Frederikshavn using low-
624 temperature geothermal energy for district heating.” *Applied Energy*, 88(2), 479-487.

625Robertson, E. C. (1988). *Thermal properties of rocks* (No. 88-441). US Geological Survey.

626Schneider, D., Strothöffer, T., & Broßmann, E. (1996). “Die 2800 m von Prenzlau oder die tiefste
627 Erdwärmesonde der Welt. *Geothermische Energie*,16, 10-12.”

628Sass, J. H., Lachenbruch, A. H., Munroe, R. J., Greene, G. W., & Moses, T. H. (1971). “Heat
629 flow in the western United States.” *Journal of Geophysical Research*, 76(26), 6376-6413.

630Sass, J. H., Galanis Jr, S. P., Lachenbruch, A. H., Marshall, B. V., & Munroe, R. J.
631 (1984). *Temperature, thermal conductivity, heat flow, and radiogenic heat production*
632 *from unconsolidated sediments of the Imperial Valley, California* (No. 84-490). US
633 Geological Survey.

634Sass, J. H., Lachenbruch, A. H., Galanis, S. P., Morgan, P., Priest, S. S., Moses, T. H., & Munroe,
635 R. J. (1994). “Thermal regime of the southern Basin and Range Province: 1. Heat flow
636 data from Arizona and the Mojave Desert of California and Nevada.” *Journal of*
637 *Geophysical Research: Solid Earth*, 99(B11), 22093-22119.

638 Śliwa, T., Gonet, A., Sapinska-Sliwa, A., Knez, D., & Jezuit, Z. (2015) Applicability of Borehole
639 R-1 as BHE for Heating of a Gas Well. In *Proceedings World Geothermal Congress*
640 *2015*.

641 Śliwa, T., Rosen, M. A., & Jezuit, Z. (2014). Use of oil boreholes in the carpathians in
642 geoennergetic systems: Historical and conceptual review. *Research Journal of*
643 *Environmental Sciences*, 8(5), 231.

644 Śliwa, T., & Kotyza, J. (2003). Application of existing wells as ground heat source for heat
645 pumps in Poland. *Applied Energy*, 74(1), 3-8.

646 State of California (2007) *California Code of Regulations*, Article 3: Requirements, Section
647 1723: Plugging and Abandonment (Publication No. PRC04). State of California. March
648 2007, p. 18 <ftp://ftp.consrv.ca.gov/pub/oil/regulations/PRC04.pdf>

649 Tester, J. W., Herzog, H. J., Chen, Z., Potter, R. M., & Frank, M. G. (1994). “Prospects for
650 universal geothermal energy from heat mining.” *Science & Global Security*, 5(1), 99-121.

651 Tester, J. W., Anderson, B. J., Batchelor, A. S., Blackwell, D. D., DiPippo, R., Drake, E. M., &
652 Petty, S. (2006). The future of geothermal energy. *Impact of Enhanced Geothermal*
653 *Systems (EGS) on the United States in the 21st Century*, Massachusetts Institute of
654 *Technology, Cambridge, MA*, 372.

655 Townend, J., & Zoback, M. D. (2004). Regional tectonic stress near the San Andreas fault in
656 central and southern California. *Geophysical Research Letters*, 31(15).

657 Williams, C. F., Grubb, F. V., & Galanis, S. P. (2004). “Heat flow in the SAFOD pilot hole and
658 implications for the strength of the San Andreas Fault.” *Geophysical Research*
659 *Letters*, 31(15).

660 Williams, Colin F. *The thermal regime of Santa Maria province, California*. No. 1995. US
661 Government Printing Office, 1994.

662 Zhai, Z., & Sharma, M. M. (2005). “A new approach to modeling hydraulic fractures in
663 unconsolidated sands.” In *SPE Annual Technical Conference and Exhibition*. Society of
664 Petroleum Engineers.

665 Zimmermann, G., & Reinicke, A. (2010). “Hydraulic stimulation of a deep sandstone reservoir to
666 develop an Enhanced Geothermal System: Laboratory and field experiments.”
667 *Geothermics*, 39(1), 70–77. <http://doi.org/10.1016/j.geothermics.2009.12.003>

668Zoback, M., Zoback, M., Eaton, J., Mount, V., & Suppe, J. (1987). “New evidence on the state
669 of stress of the San Andreas fault system.” *Science*, 238(4830), 1105-1111.
670Zui, V. I., & Martynova, O. (2015). Geothermal resources, country update for Belarus.
671 In *Proceedings, World Geothermal Congress* (p. 14).
672